Application of direct-reading and elemental carbon analysis methods to measure mass-based penetration of carbon nanotubes through elastomeric half-face and filtering facepiece respirators

Evanly Vo[a], **Ziqing Zhuang**[a], **Eileen Birch**[b], and **Quinn Birch**[b]

[a]National Institute for Occupational Safety and Health, National Personal Protective Technology Laboratory, Pittsburgh, Pennsylvania, USA

[b]National Institute for Occupational Safety and Health, Division of Applied Research and Technology, Cincinnati, Ohio, USA

Abstract

The aim of this study was to apply a direct-reading aerosol instrument method and an elemental carbon (EC) analysis method to measure the mass-based penetration of single-walled carbon nanotubes (SWCNTs) and multi-walled carbon nanotubes (MWCNTs) through elastomeric half-mask respirators (EHRs) and filtering facepiece respirators (FFRs). For the direct-reading aerosol instrument method, two scanning mobility particle sizer/aerodynamic particle sizer systems were used to simultaneously determine the upstream (outside respirator) and downstream (inside respirator) test aerosols. For the EC analysis method, upstream and downstream CNTs were collected on filter cassettes and then analyzed using a thermal-optical technique. CNT mass penetrations were found in both methods to be within the associated efficiency requirements for each type and class of the respirator models that were tested. Generally, the penetrations of SWCNTs and MWCNTs had a similar trend with penetration being the highest for the N95 EHRs, followed by N95 FFRs, P100 EHRs, and P100 FFRs. This trend held true for both methods; however, the CNT penetration determined by the direct-reading aerosol instrument method (0.009–1.09% for SWCNTs and 0.005–0.21% for MWCNTs) was greater relative to the penetration values found through EC analysis method (0.007–0.69% for SWCNTs and 0.004–0.13% for MWCNTs). The results of this study illustrate considerations for how the methods can be used to evaluate penetration of morphologically complex materials through FFRs and EHRs.

1. Introduction

Reliable test methods and test results for the evaluation and selection of respiratory protection for use in nanotechnology settings are of great interest to the health protection community. Carbon nanotubes (CNTs) are widely used in numerous industrial and biomedical products (NIOSH 2013). However, interstitial fibrosis and acute pulmonary

inflammation have been observed in CNT-exposed animal studies (Shvedova et al. 2008; Lee et al. 2010). Toxicological evidence in CNT-exposed animal studies suggests the potential for human health effects from exposure to CNTs (NIOSH 2013). The range of toxicities may depend on the CNT type (e.g., single-walled CNTs [SWCNTs] versus multi-walled CNTs [MWCNTs]) and their properties (e.g., single fibers versus agglomerated structures, purified versus raw forms, and fiber length) (Donaldson et al. 2006).

Some recent studies suggest that workers may be at risk for exposure to CNTs during the manufacture, handling, and cleanup of CNT materials (Muller et al. 2005; Dahm et al. 2015). Inhalation of aerosolized CNTs and carbon nanofibers (CNFs) is the main route of exposure and is of the greatest concern (Birch et al. 2011). To address the concern of workers exposed to CNTs, some CNT exposure limits have been proposed. The Japanese New Energy and Industrial Technology Development Organization has proposed an interim occupational exposure limit (OEL) of 21 μg/m^3 for MWCNTs (Kobayashi et al. 2009). A respirable mass-based recommended exposure limit (REL) for CNTs and CNFs, based on respirable elemental carbon (EC), was established by NIOSH: 1 μg/m^3 EC as an 8-h time-weighted average (TWA) concentration (NIOSH 2013).

With the development of exposure methods and limits for CNTs, engineering controls can be implemented and tested to monitor tasks that involve potential exposures to airborne CNTs/ CNFs, as well as to determine the suitability of different types of respiratory protection for use when engineering controls may not be available or sufficient. A NIOSH survey of US manufacturers handling carbonaceous nanomaterials indicated that 77% of the companies used some respiratory protection, such as elastomeric half-mask respirators (EHRs) and filtering facepiece respirators (FFRs; Dahm et al. 2011). Although some studies on filtration of CNTs have been reported (Seto et al. 2010; Wang 2013), these studies evaluated mechanical filters or screen filters. Recently, several CNT studies involving electret respirator filters have been reported (Vo and Zhuang 2013; Chen et al. 2014; Vo et al. 2014); however, the CNT penetration study of Chen et al. (2014) used solvents as aerosol generator fluids and focused on specific mobility equivalent diameter ranges of 20–500 nm. The respirator filtration study of Vo et al. (2014) was focused only on (1) CNT aerosol generator development to produce airborne CNTs from dry, bulk powder materials, (2) the filtration performance for FFRs using a particle count-based method, and (3) how CNTs behave relative to spherical particles collected at the same airflow rate: 85 liters per minute (LPM). Another respirator penetration study of Vo et al. (2014) was targeted toward testing FFRs using both a count-based particle concentration method and EC analysis. Currently, there is a lack of studies on: (1) CNT penetration through EHRs and (2) measurement of mass-based CNT penetration through FFRs and EHRs using a direct-reading aerosol instrument method.

The aim of this study was to compare CNT penetrations determined by direct-reading and EC methods. Mass-based penetrations and the most penetrating particle size (MPPS) of SWCNT and MWCNT through FFRs and EHRs were determined. This was the first study to: (1) apply both a direct-reading aerosol instrument and EC analysis to determine mass-based penetrations of SWCNT and MWCNT through FFRs and EHRs, and (2) obtain information on the physical structure and dimensions of upstream and downstream airborne SWCNTs and MWCNTs using transmission electron microscopy (TEM). Although a

combination of methods (e.g., for aerosol particle count, size, mass, and composition) can yield the best overall picture of worker exposure, in practice, researchers and industrial hygienists often select specific methods to target their study objectives, based on the advantages and limitations of each method. In this study, the mass-based penetration of CNTs (including CNT size distribution) through FFRs and EHRs is useful relative to the traditional, count-based method because mass-based results of direct-reading aerosol instruments (e.g., scanning mobility particle sizer [SMPS] and aerodynamic particle sizer [APS]) can be compared directly with the corresponding EC concentrations and the NIOSH REL (1 μg/m^3 as a respirable EC, 8-h TWA). Other metrics have been applied to workplace monitoring, including CNT "structure" counts determined by transmission electron microscopy (TEM; Dahm et al. 2015; Birch et al. 2016), but microscopy-based methods have limitations due to the variety and complexity of CNT products. As such, they are considered semi-quantitative (Birch et al. 2016). Nevertheless, positive correlation was found between EC and CNT structure counts (by TEM), though with considerable data scatter.

2. Materials and methods

2.1. Equipment and supplies

2.1.1. CNT aerosol respirator testing system—A CNT aerosol respirator testing system (CNT-ARTS) was previously developed (Vo and Zhuang 2013) and was used for testing of FFRs and EHRs. This testing system was capable of generating airborne CNTs from dry, bulk powder materials (Vo and Zhuang 2013). Bulk powder dispersion is more representative of workplace dispersion during handling of CNT powders (Calvert et al. 2009). Thus, a powder dispersion method is preferable to nebulizer dispersion of CNTs in a liquid suspension.

2.1.2. SWCNT and MWCNT samples—All SWCNT and MWCNT powder samples used in this study were obtained from Nanostructured & Amorphous Materials, Inc. (SWNT-1246YJS, lot 1227-090111 and MWNT-1227YJS, lot 1227-041709; Houston, TX, USA). Both materials were produced by the chemical vapor deposition (CVD) method. According to the manufacturer, the specific surface area (SSA) of the SWCNT material is >380 m^2/g and the reported purity is 90%. The average diameter varies from 1 to 2 nm and the lengths range from 1 to 3 μm. The MWCNT material has a reported purity >95%, an SSA > 40 m^2/g, average diameter between 50 and 80 nm, and lengths of 0.5–2 μm. Actual morphological and mobility-equivalent particle diameter characteristics of the test materials were determined in this study as described below.

2.1.3. Respirators—Eight combinations of respirator models involving two respirator types and two classes of filters (2 N95 FFRs, 2 P100 FFRs, 2 N95 EHRs, and 2 P100 EHRs) were selected for this study. These FFRs and EHRs were selected based on: (1) their common use in the carbonaceous nanomaterial industry (Dahm et al. 2011), (2) NIOSH certification, and (3) their commercial availability. The respirator models in each series (class of filter) were randomly assigned labels A or B (Table 1). The filter media in these respirators were electret-type filters and had a multilayer structure, and the main layers were

composed of polypropylene fibers; however, each model has a different number of layers and thickness.

2.2. Generation and characterization of airborne CNTs

SWCNT and MWCNT particles in the respirable-size range were generated according to the method of Vo and Zhuang (2013). The detailed generation procedure for airborne SWCNTs and MWCNTs has been described previously (Vo et al. 2014).

An ultrafine condensation particle counter (UCPC, model 3776, TSI Inc., Shoreview, MN, USA) was used to track the minute-by-minute concentration variations of SWCNT or MWCNT particles in the test chamber to ensure that the CNT-ARTS was: (1) generating a sufficient amount of SWCNT and MWCNT particles required for testing the high efficiency P100 FFRs and EHRs (Vo and Zhuang 2013) and (2) maintaining a stable SWCNT or MWCNT output concentration in the test chamber during a test period.

The SMPS and APS systems (Figure 1, SMPS-APS system 1) were used to characterize the size distributions of airborne SWCNTs and MWCNTs inside the test chamber. The SMPS consists of an electrostatic classifier (TSI Model 3080) with a differential mobility analyzer (DMA, TSI Model 3081), a condensation particle counter (CPC, TSI Model 3772), and a data-collection computer with an aerosol instrument manager (AIM) software (Version 9.0; TSI). The AIM software (Version 9.0) was also used for the APS. The SMPS parameters were set at 0.3 LPM for aerosol sample flow, 3 LPM for sheath flow, and 2 min scan time for each sample. Operating the SMPS aerosol flow at 0.3 LPM yielded a size distribution range approximately from 20 to 700 nm in 64 size channels per decade. Although the densities of the stock-powder SWCNTs and MWCNTs are 2.1 g/cm^3, their dispersion densities were estimated to be approximately 0.006 g/cm^3 and this density value was used for the SMPS parameter input. Two minute-sample scan time and the CNT density value of 0.006 g/cm^3 were also used for the APS. The APS size distribution ranged from 0.5 to 20 μm in 32 size channels per decade. The SMPS and APS output data in this study were reported in the "mass-based concentration" mode by setting the mass unit ($\mu g/m^3$) for the vertical axis as a function of particle diameter unit (nm) for the horizontal axis using the AIM Version 9.0 software. The combination of the SMPS (electrical mobility size distribution) and APS data (aerodynamic size distribution) into a single size distribution (20–20,000 nm) was performed according to the method of Khlystov et al. (2004) by calculating the ratio of the overlapping size range between 500 and 700 nm. In this article, all SMPS–APS size distributions were combined and reported in the mobility equivalent diameter as a function of the mass-based concentration ($\mu g/m^3$).

2.3. Measuring mass-based CNT penetration using a direct-reading instrument method

Before each penetration experiment, each FFR or EHR was sealed to the face of the head form, with silicone, and a leakage test was conducted according to the method of Vo and Zhuang (2013). Thus, face-seal leakage was not a respirator route of entry for this study.

The penetration procedure was carried out at a constant flow rate of 30 ± 1 LPM to simulate inhalation at a normal work rate (Clayton et al. 2002). CNTs outside each FFR or EHR (Figure 1, SMPS-APS system 1) were designated as upstream particles, and CNTs that

penetrated through the respirator (Figure 1, SMPS-APS system 2) were designated as downstream particles. The mass-based concentration (μg/m^3) was measured with the SMPS–APS system based on the integrated volume concentration and an assumed bulk aerosol density (Shen et al. 2002). The mass-based upstream and downstream samples were measured simultaneously using the SMPS–APS system 1 and system 2, respectively (Figure 1). The combination of each SMPS–APS data set of mass-based upstream and downstream samples was measured as described in the "generation and characterization of airborne CNTs" section. This method allows measuring the concentration and size distribution of airborne CNT particles in a wide size range from 20 to 20,000 nm into a single plot, and was used for all SMPS-APS data sets from this study. Thus, the mass-based CNT penetration through respirators using a direct-reading aerosol instrument method was determined based on the mass-based downstream and upstream concentrations recorded in each SMPS–APS experimental data set. The mass-based penetrations for each respirator model in the direct-reading method were reported as: (1) penetration as a function of individual particle size and (2) penetration based on the summation of particle concentration across the full size range measured. Penetration (P_i in %) as a function of individual particle size was calculated as a ratio of the downstream and upstream concentrations:

$$P_i = (C_{\text{down}} / C_{\text{up}}) \times 100, \quad [1]$$

where C_{down} is the mean downstream mass-based CNT concentration at each particle size and C_{up} is the upstream CNT concentration at each particle size.

The summation penetration (P_s in %) of all particle sizes, across the full size range, was calculated as

$$P_s = \left(\sum C_{\text{down}} / \sum C_{\text{up}} \right) \times 100, \quad [2]$$

where ΣC_{down} is the total downstream mass-based CNT concentration and ΣC_{up} is the total upstream concentration.

2.4. Measuring mass-based CNT penetration using EC analysis

2.4.1. Collection of CNT samples for EC analysis—The penetration experiments for the EC analysis method were carried out using the same penetration procedure as described in the direct-reading instrument method; however, in this experiment, all samples of SWCNTs and MWCNTs were collected with filter cassettes (3-piece preloaded cassette containing a 37-mm diameter quartz-fiber filter, model # 225-401; SKC Inc., Eighty Four, PA, USA) for EC analysis. For each FFR and EHR model, triplicate sets of upstream and downstream CNT samples were collected simultaneously on filters using an in-house vacuum system (Figure 1, 1A–1D, and Figure 1, 2A–2C). Before selecting the airflow rates for upstream and downstream sample collection, the performance of the quartz filters was checked using different airflow rates (1, 3, 5, 10, 15, and 20 LPM). The following results

were obtained: (a) airflow rates of 1, 3, and 5 LPM did not affect the particle collection efficiency of the quartz filters (an airstream passed through the filter media was monitored using a CPC and no particle counts were detected); (b) an airflow rate of 10 LPM also did not affect the quartz-filter efficiency, but an uneven sample deposition across the filter was observed; (c) airflow rates of 15 and 20 LPM did minor damage to the quartz filter, resulting in some particles being detected by a downstream CPC. For this reason, these higher flow rates (10 LPM) were not used. In summary, the different air-flow rates (3 LPM) used for this study did not affect the collection efficiency of the quartz filter and yielded uniform sample deposition across the filter. Different airflow rates and sampling times were used for collecting upstream and downstream samples in order to achieve the sample-collection requirements within the normal work period (4 h). For the upstream CNT samples, the airflow rate was set to 0.5 LPM and the collection time was 3 min for each sample. For the downstream samples, the airflow rate was set to 3 LPM and the collection time was 90 and 180 min for respirator class N95 and P100, respectively. After completing each sample collection, the filter cassette was covered with the cassette cap and stored at room temperature prior to the EC analysis.

2.4.2. Quantitative analysis of CNTs using EC analysis—Organic carbon (OC) and EC analyses were performed at a NIOSH laboratory (under Dr. Birch's supervision) according to NIOSH Method 5040 (Birch and Cary 1996; NIOSH 2003, 2013, 2016; Birch et al. 2011), with minor modifications (Birch et al. 2011; NIOSH 2013, 2016; Dahm et al. 2015). Specifically, for application to CNTs/CNFs, a manual OC-EC split is assigned. To optimize the split and ensure complete oxidation, bulk materials are analyzed to check their thermal profiles. In some cases (not this study), depending on the sample, adjustment of the temperature program (e.g., higher temperature and/or longer oxidation period) may be required (Birch et al. 2011; Doudrick et al. 2012; NIOSH 2013, 2016; Dahm et al. 2015). In this study, sample collection was in an enclosed chamber with filtered air, and the OC (and trace metal) contents of the bulk materials were negligible. Thus, the analysis was straightforward because CNTs were the only source of EC in the filter samples. Further details on thermal-optical analysis of the EC contents of upstream and downstream filter samples collected for respirator penetration studies have been described previously (Vo et al. 2014).

2.4.3. Measuring mass-based CNT penetration using EC analysis—The mass-based SWCNT and MWCNT penetrations were calculated as described in Equation (2); however, in the EC-analysis penetrations, ΣC_{down} is the downstream EC concentration [total EC on the 37-mm diameter filter per cubic meter ($\mu g/m^3$) of downstream air containing CNT] and ΣC_{up} is the upstream EC concentration (total EC on the filter that sampled upstream air).

2.5. Transmission electron microscopy sample collection and analysis

To obtain the physical structure and dimensions of particles, samples of the SWCNT and MWCNT aerosols were collected for analysis by TEM. The general information of TEM sample collection and analysis methods are provided elsewhere (Han et al. 2008; Bello et al. 2009; Lee et al. 2010; Dahm et al. 2015). In this study, TEM samples were collected with

open-face, 25-mm filter cassettes containing methyl cellulose ester (MCE) filters. A media blank was provided with each filter set to check for filter contamination. The filters were prepared and analyzed on a JEOL 2100F TEM (JEOL USA, Inc., Peabody, MA, USA) using a modified NMAM 7402 (Dahm et al. 2015). Modifications relate mainly to elimination of steps required to identify and count asbestos fibers. A different counting approach was needed for CNT particles, which occur mainly as complex, agglomerated structures. For the analysis, three 3-mm, copper TEM grids from each sample were examined at low magnification to determine loading and ensure sample preparation quality, and representative images of each sample were collected.

2.6. Data analysis

All average and standard deviation data were analyzed using Microsoft Excel 2010 software (Microsoft Corporation, Redmond, WA, USA). Paired *t*-tests with two-tailed distribution were performed to analyze the differences in the percent mass penetrations between two methods and between SWCNT and MWCNT types, for each respirator model, also using Microsoft Excel 2010. *P*-values of < 0.05 were considered significant.

3. Results

3.1. Generation and characterization of airborne SWCNTs and MWCNTs

The mean output SWCNT and MWCNT concentration levels in the test chamber were found to be 1.05×10^5 ($\pm 6.48 \times 10^3$) for SWCNTs and 1.36×10^5 ($\pm 7.62 \times 10^3$) particles/cm^3 for MWCNTs ($n = 3$). The results show that the CNT-ARTS was capable of generating a consistent average concentration of SWCNT or MWCNT over the 4-h test period at levels sufficient for respirator testing (3×10^4 particles/cm^3 required for testing P100 FFRs and EHRs) (Vo and Zhuang 2013).

Size distributions of output SWCNTs and MWCNTs in the test chamber were also characterized using the SMPS-APS system. The size distributions, which express the mass-based concentration ($\mu g/m^3$) of airborne CNTs as a function of particle diameter (mobility equivalent diameter), are shown in Figure 2. Results show that 99% of the particles measured were between 150 and 2300 nm for SWCNTs (Figure 2, solid line). The mass median mobility equivalent diameter (MMMED) was 598 nm with a geometric standard deviation (GSD) of 1.40 for airborne SWCNTs. For MWCNTs, 99% of the particles measured were between 180 and 3100 nm (Figure 2, dashed line). The MMMED was 634 nm with a GSD of 1.48 for airborne MWCNTs. Example TEM images of the upstream and downstream aerosolized SWCNT and MWCNT particles are shown in Figure 3. Based on the TEM results, most of the upstream SWCNT particles were agglomerates, with typical sizes of about 1 μm up to >10 μm (Figure 3a). The larger (>10 μm) particles appeared as complex structures that may be multiple, overlapping particles. The most common size bin for the downstream SWCNTs was 2–5 μm (Figure 3b). A few isolated fibers having nanoscale diameters also were found but were relatively few. For MWCNT particles, the overall envelope size of the upstream MWCNT particle agglomerates ranged from the sub-μm scale to about 10 μm, with most being in the 1–5 μm range (Figure 3c). A few isolated fibers having nanoscale diameters also were found (Figure 3c). The downstream MWCNT

particles typically were smaller, with a maximum size of about 5 μm and >60% of the counted particles in the sub-μm range (agglomerates and a few nanoscale fibers) (Figure 3d).

3.2. Measuring mass-based CNT penetration using a direct-reading instrument method

Percent mass-based penetration values for the eight respirator models at constant flow rates of 30 LPM as a function of individual particle size are shown in Figure 4. For SWCNTs, the MPPS through the four FFR models was found to be in the range of 35–240 nm (35–180, 45–240, 40–170, and 40–170 nm for N95-A FFRs, N95-B FFRs, P100-A FFRs, and P100-B FFRs, respectively; Figure 4), while the MPPS through the four EHR models was found to be in the range of 20–170 nm (30–170, 30–170, 35–170, and 40–170 nm for N95-A, N95-B, P100-A, and P100-B EHRs, respectively; Figure 4). For MWCNTs, the MPPS through the four FFR models was found to be in the range of 25–510 nm (25–510, 25–510, 35–240, and 25–240 nm for N95-A, N95-B, P100-A, and P100-B FFRs, respectively; Figure 4), while the MPPS through the four EHR models was found to be in the range of 20–350 nm (20–350, 20–350, 25–350, and 25–500 nm for N95-A, N95-B, P100-A, and P100-B EHRs, respectively; Figure 4).

Percent mass-based SWCNT and MWCNT penetrations based on the summation of particle concentrations across the size range measured for the eight tested respirator models are shown in Table 1. For the percent SWCNT penetration, average percent penetrations were the highest for the N95 EHRs (0.88–1.09%), followed by N95 FFRs (0.23–0.48%), P100 EHRs (0.017–0.019%), and P100 FFRs (0.009–0.012%) (Table 1). The paired t-tests ran for different respirator models within each filter class (N95-A versus N95-B or P100-A versus P100-B) revealed all P-values > 0.05. This indicates that penetrations were not significantly different between respirator models within each filter class; however, the mass-based penetrations for N95 respirator class were greater compared with the values for P100 respirator class (all P-values < 0.05). This indicates that penetrations were significantly different between two different respirator classes.

For the percent MWCNT penetration, average percent penetrations were the highest for the N95 EHRs (0.18–0.21%), followed by N95 FFRs (0.11–0.15%), P100 EHRs (0.008–0.009%), and P100 FFRs (0.005–0.007%) (Table 1). In general, the mass-based penetrations for the N95 respirator class were greater than the values for the P100 class (all P-values < 0.05). This indicates that penetrations were significantly different between two respirator classes; however, penetrations were not significantly different between respirator models within each filter class (all P-values > 0.05).

3.3. Measuring mass-based CNT penetration using elemental carbon analysis

Upstream and downstream samples of SWCNTs and MWCNTs at 30 LPM constant flow rates were collected for the Method 5040 analysis. All upstream and downstream samples of SWCNTs and MWCNTs were found to deposit evenly across the filter. Thus, a single punch (a 1.5-cm^2 sample portion) from each quartz filter was analyzed for EC and was representative of the entire deposit. The total EC on the filter was calculated as: [EC (μg/cm^2) on the 1.5-cm^2 sample portion – EC blank] times the total deposit area (excluding the area covered by the rim of the cassette piece that compresses against the filter. The deposit

diameter was about 33 mm, corresponding to a deposit area of about 8.55 cm^2). For comparison with data from the direct-reading instrument, all upstream and downstream EC results (μg/cm^2) were converted to air concentrations (μg/m^3). Sample calculations of upstream and downstream EC concentrations are shown in Table 2. Mean upstream and downstream concentrations of SWCNTs and MWCNTs collected on quartz filters for all eight respirator models are shown in Table 1.

The percent mass-based penetration values of SWCNTs for the eight FFR and EHR models are shown in Table 1. Based on EC results, average percent penetrations of SWCNTs were the highest for the N95 EHRs (0.40–0.69%), followed by N95 FFRs (0.18–0.29%), P100 EHRs (0.011–0.014%), and P100 FFRs (0.007–0.008%) (Table 1). The paired t-tests for different respirator models within each filter class (N95-A versus N95-B or P100-A versus P100-B) revealed all P-values > 0.05. This indicates that penetrations were not significantly different between respirator models within each filter class of each respirator type (FFR or EHR); however, the mass-based penetrations for the N95 respirator class were greater relative to the values for the P100 class (all P-values < 0.04). This indicates that penetrations were significantly different between the two respirator classes.

The percent mass-based penetration values of MWCNTs for the eight FFR and EHR models are shown in Table 1. Average percent penetrations were the highest for the N95 EHRs (0.12–0.13%), followed by N95 FFRs (0.04–0.05%), P100 EHRs (0.006–0.008%), and P100 FFRs (0.004–0.005%) (Table 1). In general the penetrations for the N95 respirator class were greater than those for the P100 class (all P-values < 0.05). This indicates that penetrations were significantly different between the two different respirator classes; however, penetrations were not significantly different between respirator models within each filter class (all P-values > 0.05).

3.4. Comparison of the direct-reading instrument and EC analysis methods

Table 1 shows the mass-based SWCNT and MWCNT penetrations through FFRs and EHRs, based on the direct-reading instrument and EC analysis methods, respectively. In general, the penetrations of SWCNTs and MWCNTs had a similar trend for both methods, with penetration being the highest for the N95 EHRs, followed by N95 FFRs, P100 EHRs, and P100 FFRs. However, the CNT penetrations determined by the direct-reading instrument (0.009–1.09% for SWCNTs and 0.005–0.21% for MWCNTs) were greater relative to the penetration values found through EC analysis (0.007–0.69% for SWCNTs and 0.004–0.13% for MWCNTs). For the combination of both N95- and P100-respirator classes, the penetrations for SWCNTs in the direct-reading instrument method were not significantly different compared with the values for SWCNTs in the EC analysis method (P-values > 0.07), while the penetrations for MWCNTs in the direct-reading instrument method were significantly different compared with the values for MWCNTs in the EC analysis method (P-values < 0.04). Within the N95-respirator class, the results show that the SWCNT penetrations were not significantly different between the direct-reading instrument and EC analysis methods; however, there were significant differences between two methods for MWCNTs (P-values   0.003). Interestingly, when comparing the CNT penetrations through the P100-respirator class between the two methods, the paired t-tests for both SWCNT and

MWCNT penetrations revealed all P-values < 0.02. This indicates that both SWCNT and MWCNT penetrations were significantly different between the two methods for P100-respirator class.

4. Discussion

The CNT-ARTS was capable of producing and maintaining stable airborne SWCNT and MWCNT concentration levels during a 4-h test period for the respirator penetration study. Size distributions, which express the mass-based concentration (μg/m^3) as a function of particle diameter, showed that the MPPS for CNTs through the eight respirator models, which have electret filters, was in the range of 30–240 nm and 20–510 nm for SWCNTs and MWCNTs, respectively. Two possible explanations for the larger size range of the MPPS in MWCNTs when compared to SWCNTs are: (i) the MWCNT outputs (upstream particles) were larger size (MMMED = 634 nm) than the SWCNT particle outputs (MMMED = 598 nm) and (ii) the respirator-filter capture efficiency of SWCNTs and MWCNTs might differ due to their different particle shapes and sizes as shown in their TEM images.

Comparison of the mass-based penetrations between SWCNTs and MWCNTs based on the summation of particle concentrations across the size range in the direct-reading instrument method indicated that different CNT types and different respirator models yielded different penetrations. In general, both SWCNT and MWCNT aerosol types had a similar trend in the penetration, and average penetrations were the highest for the N95 EHRs, followed by N95 FFRs, P100 EHRs, and P100 FFRs. Although the penetrations for SWCNTs were not significantly different compared with the values for MWCNTs for the N95-class respirators (P-values > 0.06), there were significantly different penetrations between SWCNTs and MWCNTs for the P100-class respirators (P-values < 0.02). A possible explanation for this is that the output aerosolized SWCNTs had a smaller size than the aerosolized MWCNTs. Thus, the capture efficiency of the respirator filter would be increased due to surface interaction, interception, and inertial impaction for the MWCNTs with their larger surface areas and complex shape (Wang and Pui 2009; Wang et al. 2011a). Within each CNT aerosol type (SWCNT or MWCNT), the results show that penetrations were not significantly different between two models in each respirator class (N95-A versus N95-B; P100-A versus P100-B). Interestingly, our previous study shows that the count-based penetrations for two other different models in the N95 respirator class were significantly different (Vo et al. 2014). A possible explanation for the different penetrations in our previous study is that both of the tested N95 FFR models have different outer layer filter materials (one has a hydrophobic outer layer and the other model has a hydrophilic outer layer), while both N95 FFR models used in this study have the same hydrophobic outer layer. For different filter classes (N95 FFRs versus P100 FFRs; N95 EHRs versus P100 EHRs), penetrations were significantly different between them. The filter properties (polypropylene fibers and electrical charges), numbers of filter layers, total filter thickness, and the surface interaction with CNTs may contribute to the significant differences between different filter classes. In general, the relative penetrations found for the different classes (mass-based penetrations of CNTs: 0.18–1.09% for N95 and 0.004–0.019% for P100) are expected (the acceptable penetrations of these respirator classes: 5% for N95 and 0.03% for P100 FFRs).

Interestingly, the EC-based respirator penetrations of both SWCNT and MWCNT aerosols had a similar trend to those found in the direct-reading instrument method. The average penetrations were highest for the N95 EHRs, followed by N95 FFRs, P100 EHRs, and P100 FFRs. For the SWCNT and MWCNT materials tested in this study, the EC results show penetrations of SWCNT aerosols that are always higher than MWCNT penetrations when comparing the same respirator models. The paired *t*-tests for the penetrations between SWCNT and MWCNT in the EC analysis method revealed all *P*-values < 0.05. This indicates that the penetration values for SWCNTs were significantly different than those for MWCNTs, based on EC analysis. However; when comparing the penetration levels in detail between the two methods, penetration based on the direct-reading instrument method was consistently higher than that based on EC mass for all FFR and EHR models. Possible explanations for the larger penetrations found by the direct-reading aerosol instrument method are: (1) the estimated values of bulk-aerosolized CNT density for both SWCNTs and MWCNTs and (2) the integrated volume concentration for both SWCNTs and MWCNTs based on mobility equivalent diameters of their non-spherical form. An additional possible explanation for the different penetrations between the two methods is that different sampling times for upstream and downstream EC samples could yield different mass concentrations for the upstream and downstream samples due to concentration fluctuations over the different sampling periods.

5. Conclusions

Direct-reading aerosol instruments and EC analysis were applied to determine mass-based penetrations of SWCNTs and MWCNTs through eight FFR and EHR models. A mass-based measure by direct-reading instruments is more useful than the traditional, count-based method because the results can be compared directly with the corresponding EC concentrations and NIOSH REL. Results of both methods show that the penetrations of the SWCNTs and MWCNTs evaluated in this study have a similar trend, being highest for the N95 EHRs, followed by N95 FFRs, P100 EHRs, and P100 FFRs; however, CNT penetrations determined by the direct-reading method were greater relative to those found through EC analysis, which likely relates to particle structure and density. Collection of TEM samples upstream and downstream of the respirator assists data interpretation by providing complementary information on particle size and structure, and showing the types of particles that penetrate the respirator. Based on these promising results, a combination of direct-reading and filter-based methods (EC and others) also could be applied to other types of nanomaterials (e.g., carbon blacks, Ti_2O, $CaCO_3$, SiO_2, and Al_2O_3, etc.) to improve mass-based filter penetration measurements.

Institute for Occupational Safety and Health (NIOSH). Mention of company names or products does not constitute endorsement by NIOSH.

References

Bello D, Wardle BL, Yamamoto N, Guzman de Villoria R, Garcia E, Hart A, Ahn K, Ellenbecker MJ, Hallock M. Exposure to Nanoscale Particles and Fibers During Machining of Hybrid Advanced Composites Containing Carbon Nanotubes. J Nanopart Res. 2009; 11:231–249.

Birch ME, Cary RA. Elemental Carbon-Based Method for Monitoring Occupational Exposures to Particulate Diesel Exhaust. Aerosol Sci Technol. 1996; 25:221–241.

Birch ME, Ku BK, Evans DE, Ruda-Eberenz T. Exposure and Emissions Monitoring During Carbon Nanofiber Production. Part I: Elemental Carbon and Iron-Soot Aerosols. Ann Occup Hyg. 2011; 55:1016–1036. [PubMed: 21965464]

Birch, ME., Wang, C., Fernback, JH., Feng, A., Birch, QT., Dozier, AK. Workplace Monitoring of Airborne Carbon Nanomaterials by HRTEM. Proceedings of the Microscopy and Microanalysis Conference; Columbus, OH. July 24–28; 2016.

Calvert G, Ghadiri M, Tweedie R. Aerodynamic Dispersion of Cohesive Powders: A Review of Understanding and Technology. Adv Powder Tech. 2009; 20:4–16.

Chen SC, Wang J, Bahk YK, Fissan H, Pui YHD. Carbon Nanotube Penetration Through Fiberglass and Electret Respirator Filter and Nuclepore Filter Media: Experiments and Models. Aerosol Sci Technol. 2014; 48:997–1008.

Clayton MP, Bancroft B, Rajan B. A Review of Assigned Protection Factors of Various Types and Classes of Respiratory Protective Equipment with Reference to Their Measured Breathing Resistances. Ann Occup Hygiene. 2002; 46:537–547.

Dahm MM, Schubauer-Berigan MK, Evans DE, Birch ME, Fernback JE, Deddens JA. Carbon Nanotube and Nanofiber Exposure Assessments: An Analysis of 14 Site Visits. Ann Occup Hyg. 2015; 59(6):705–723. [PubMed: 25851309]

Dahm MM, Yencken M, Schubauer-Berigan M. Exposure Control Strategies in the Carbonaceous Nanomaterial Industry. J Occup Env Med. 2011; 53:S68–S73. [PubMed: 21654421]

Donaldson K, Aitken R, Tran L, Stone V, Duffin R, Forrest G, Alexxander A. Carbon Nanotubes: A Review of their Properties in Relation to Pulmonary Toxicology and Workplace Safety. Toxicol Sci. 2006; 92:5–22. [PubMed: 16484287]

Doudrick K, Herckes P, Westerhoff P. Detection of Carbon Nanotubes in Environmental Matrices Using Programmed Thermal Analysis. Environ Sci Technol. 2012; 46:12246–12253. [PubMed: 22663014]

Han JH, Lee EJ, Lee JH, So KP, Lee YH, Bae GN, Lee SB, Ji JH, Cho MH, Yu IJ. Monitoring Multi-Walled Carbon Nanotube Exposure in Carbon Nanotube Research Facility. Inhal Toxicol. 2008; 20:741–749. [PubMed: 18569096]

Khlystov A, Stanier C, Pandis SN. An Algorithm for Combining Electrical Mobility and Aerodynamic Size Distributions Data when Measuring Ambient Aerosol. Aerosol Sci Technol. 2004; 38:229–238.

Kobayashi, N., Kishimoto, A., Ogura, I. Risk Assessment of Manufactured Nanomaterials: Carbon Nanotubes (CNTs). In: Nakanishi, J., editor. Interim Report. 2009. Issued on October 16, 2009Executive summary

Lee JH, Lee SB, Bae GN, Jeon K, Yoon J, Ji J, Sung J, Lee BG, Lee JH, Yang J, Kim H, Kang C, Yu I. Exposure Assessment of Carbon Nanotube Manufacturing Workplaces. Inhal Toxicol. 2010; 22:369–381. [PubMed: 20121582]

Muller J, Huaux F, Moreau N, Misson P, Heilier JF, Delos M, Arras M, Fonseca A, Nagy JB, Lison D. Respiratory Toxicity of Multi-Wall Carbon Nanotubes. Toxicol Appl Pharmacol. 2005; 207:221–231. [PubMed: 16129115]

NIOSH. NIOSH Manual of Analytical Methods. 4. Cincinnati, OH: U.S. Department of Health and Human Services, Public Health Service, Centers for Disease Control and Prevention, National Institute for Occupational Safety and Health, DHHS (NIOSH); 2003. Diesel Particulate Matter (As Elemental Carbon): Method 5040 (Supplement Issued 3/15/03). Publication No. 94–113

Zumwalde, R.Kuempel, E.Birch, ME.Trout, D., Castranova, V., editors. NIOSH. Current Intelligence Bulletin 65: Occupational Exposure to Carbon Nanotubes and Nanofibers. Cincinnati, OH: U.S. Department of Health and Human Services, Centers for Disease Control and Prevention, National Institute for Occupational Safety and Health, DHHS (NIOSH); 2013. Publication No. 2013–145

NIOSH. Chapter DL: Monitoring of Diesel Particulate Exhaust in the Workplace. In: Birch, ME., editor. NIOSH Manual of Analytical Methods (NMAM). 5. Cincinnati, OH: U.S. Department of Health and Human Services, Centers for Disease Control and Prevention, National Institute for Occupational Safety and Health, DHHS (NIOSH); 2016. Available at http://www.cdc.gov/niosh/nmam/

Seto T, Furukawa T, Otani Y, Endo S. Filtration of Multi-Walled Carbon Nanotube Aerosol by Fibrous Filters. Aerosol Sci Technol. 2010; 44:734–740.

Shen S, Jaques PA, Zhu Y, Geller MD, Siuotas C. Evaluation of the SMPS-APS System as a Continuous Monitor for Measuring PM2.5, PM10 and Coarse PM2.5–10. Atmos Environ. 2002; 36:3939–3950.

Shvedova AA, Kisin ER, Murray AR, Johnson VJ, Gorelik O, Arepalli S, Hubbs AF, Mercer RR, Keohavong P, Sussman N, Jin J, Yin J, Stone S, Chen BT, Deye G, Maynard A, Castranova V, Baron PA, Kagan VE. Inhalation vs. Aspiration of Single-Walled Carbon Nanotubes in C57BL/6 Mice: Inflammation, Fibrosis, Oxidative Stress, and Mutagenesis. Am J Physiol Lung Cell Mol Physiol. 2008; 295:L552–L565. [PubMed: 18658273]

Vo E, Zhuang Z. Development of a New Test System to Determine Penetration of Multi-Walled Carbon Nanotubes through Filtering Facepiece Respirators. J Aerosol Sci. 2013; 61:50–59. [PubMed: 26166842]

Vo E, Zhuang Z, Birch E, Zhao Q, Horvatin M, Liu Y. Measurement of Mass-Based Carbon Nanotube Penetration through Filtering Facepiece Respirator Filtering Media. Ann Occup Hygiene. 2014; 58:646–656.

Wang J. Effects of Particle Size and Morphology on Filtration of Airborne Nanoparticles. KONA Powder Particle J. 2013; 30:256–266.

Wang J, Kim SC, Pui DYH. Measurement of Multi-Wall Carbon Nanotube Penetration Through a Screen Filter and Single-Fiber Analysis. J Nanopart Res. 2011a; 13:4565–4573.

Wang J, Pui DYH. Numerical Investigation of Filtration by Fibers with Elliptical Cross-Sections. J Nanopart Res. 2009; 11(1):185–196.
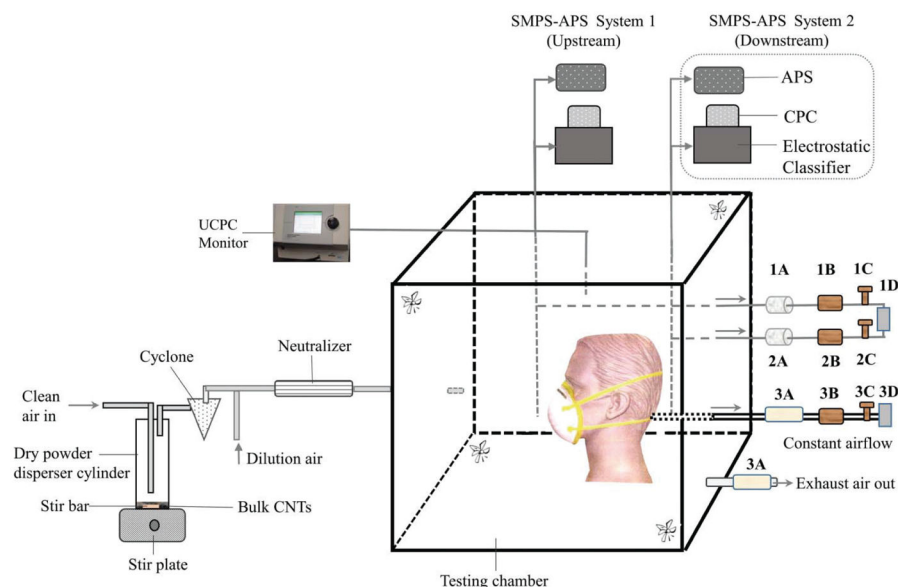
Figure 1.
Schematic diagram of CNT-ARTS, including direct-reading instruments (SMPS-APS systems 1 and 2) and a sample collection system for the EC analysis method: apparatus for upstream sample (filter cassette, 1A; mass flow meter, 1B; air regulator, 1C; in-house vacuum, 1D), apparatus for downstream sample (filter cassette, 2A; flow meter, 2B; air regulator, 2C; vacuum, 1D), and a constant airflow system (HEPA filter, 3A; flow meter, 3B; air regulator, 3C; vacuum, 3D).
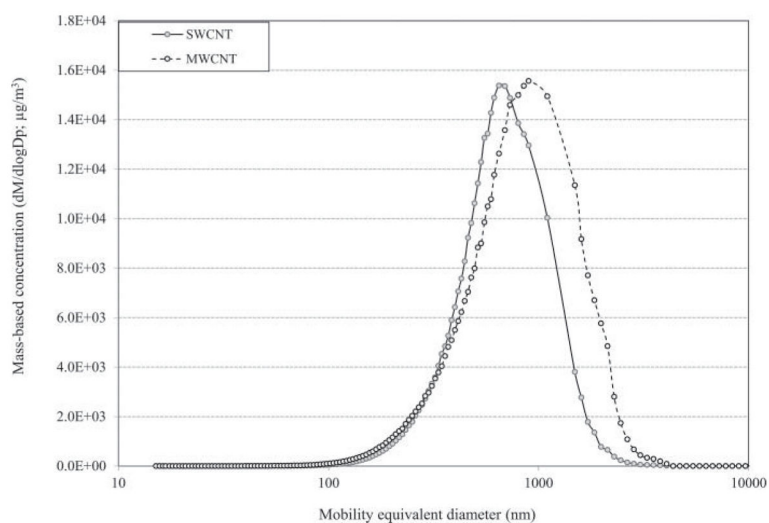
Figure 2.
Size distribution of airborne SWCNTs (solid line) and MWCNTs (dashed line) in the testing chamber measured using the combined SMPS-APS method.
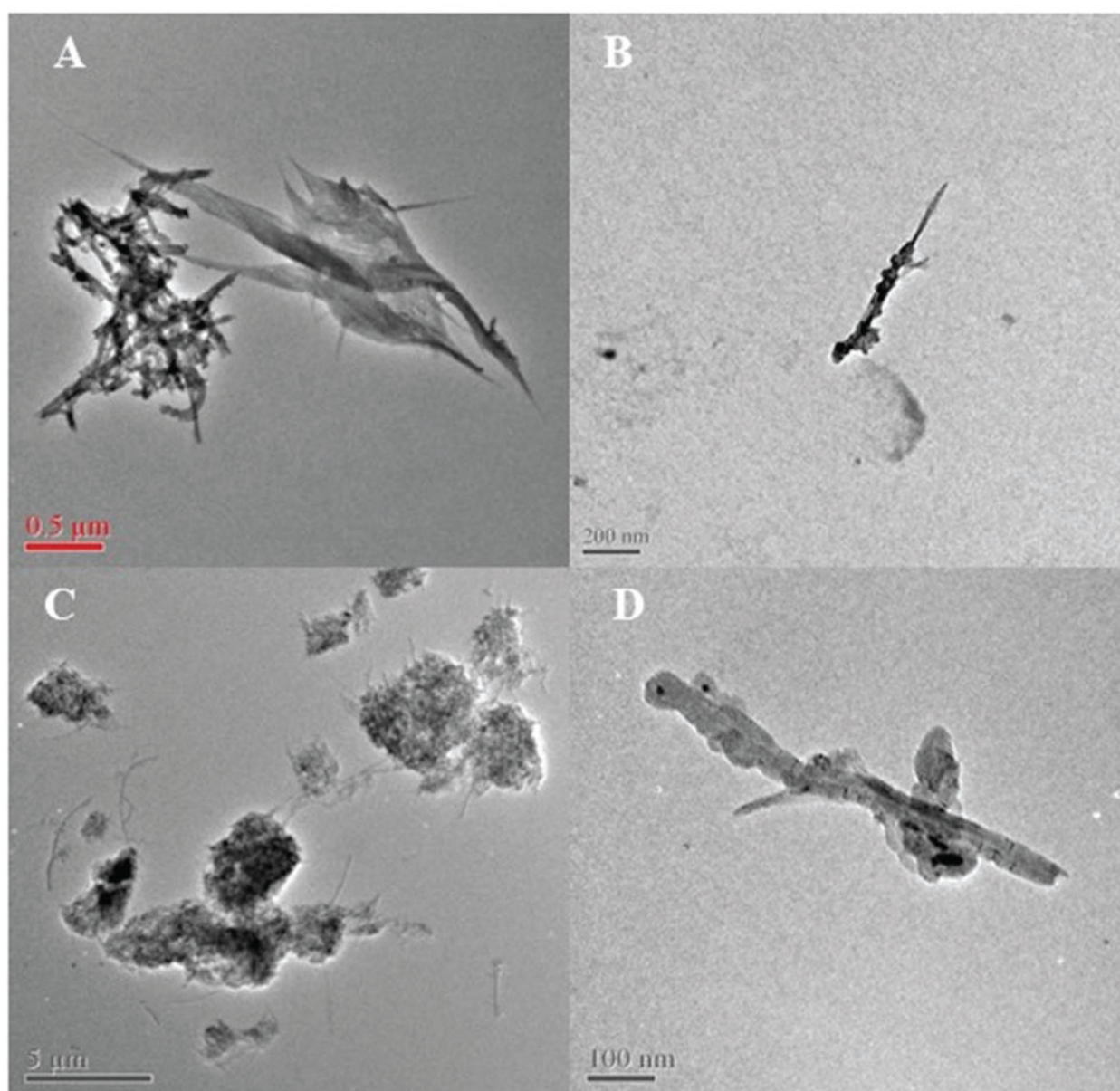
Figure 3.
TEM images of the upstream and downstream CNT particles: upstream aerosolized SWCNT particles collected in the test chamber (a); downstream SWCNT particle collected inside the respirator (b); upstream aerosolized MWCNT particles (c); downstream MWCNT particle (d).
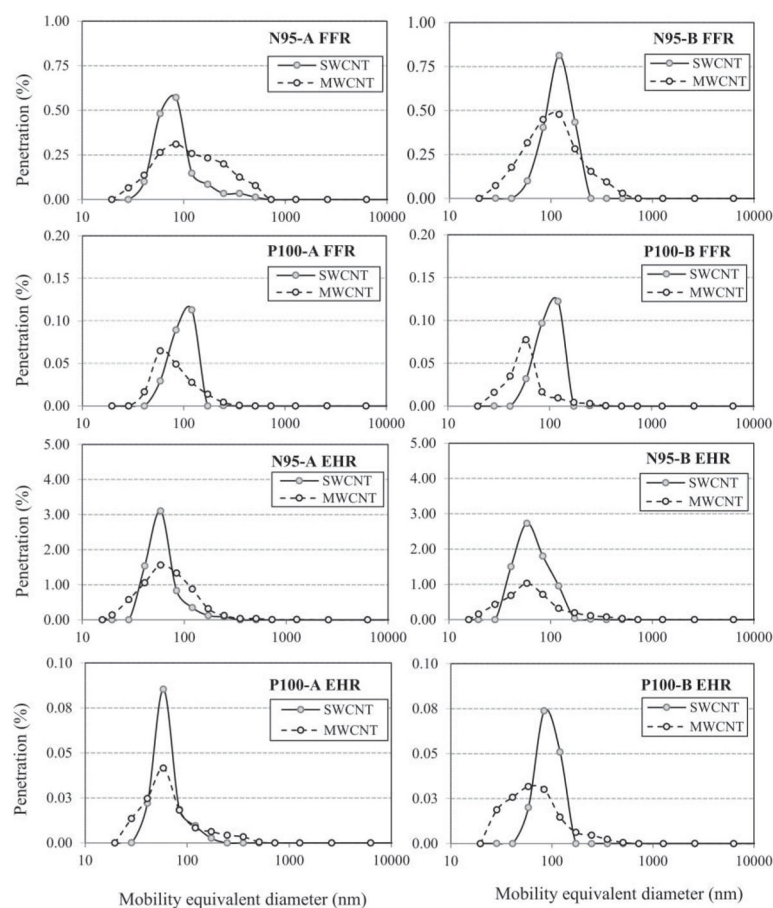
Figure 4.
Mean SWCNT and MWCNT penetrations (mass-based penetration; $n = 3$ for each model) through the tested FFRs and EHRs as a function of individual particle size measured using the SMPS-APS method.

Table 1

Mass-based SWCNT and MWCNT penetrations through FFRs and EHRs measured using direct-reading and elemental carbon analysis methods.

Respirator type	Class of filter	Respirator model	SWCNT penetrations measured by direct-reading and EC methods		MWCNT penetrations measured by direct-reading and EC methods	
			SWCNT penetration[a] by direct-reading method (%)	SWCNT penetration[a] by EC method (%)	MWCNT penetration[a] by direct-reading method (%)	MWCNT penetration[a] by EC method (%)
FFRs	N95	N95-A	0.23 ± 0.06	0.18 ± 0.06	0.11 ± 0.03[c]	0.04 ± 0.01
		N95-B	0.48 ± 0.16	0.29 ± 0.09	0.15 ± 0.05[c]	0.05 ± 0.01
	P100	P100-A	0.009 ± 0.002[b]	0.007 ± 0.002	0.005 ± 0.002[c]	0.004 ± 0.001
		P100-B	0.012 ± 0.003[b]	0.008 ± 0.002	0.007 ± 0.002[c]	0.005 ± 0.002
EHRs	N95	N95-A	1.09 ± 0.36	0.69 ± 0.23	0.21 ± 0.07[c]	0.13 ± 0.04
		N95-B	0.88 ± 0.25	0.40 ± 0.14	0.18 ± 0.05[c]	0.12 ± 0.04
	P100	P100-A	0.019 ± 0.007[b]	0.014 ± 0.005	0.009 ± 0.002[c]	0.008 ± 0.003
		P100-B	0.017 ± 0.006[b]	0.011 ± 0.003	0.008 ± 0.002[c]	0.006 ± 0.002

[a] Mean value ± relative standard deviation (n = three replicate tests);

[b] significantly different from SWCNT penetration data in the EC analysis method for the P100-respirator class;

[c] significantly different from MWCNT penetration data in the EC analysis method for both: the P100-respirator class and the combination of N95- and P100-respirator classes.

Table 2

Sample calculations of upstream and downstream EC concentrations ($\mu g/m^3$).

FFR model	CNT sample	Flow rate (LPM)	Sampling time (min)	EC on the sample portion ($\mu g/cm^2$)[a]	Total EC (CNTs) on filter (μg)[b]	CNT concentration ($\mu g/L$)[c]	CNT concentration ($\mu g/m^3$)[d]
N95 FFR	Upstream	0.5	3	3.49	29.84	19.89	19,890
	Downstream	3.0	90	0.93	7.95	0.03	30

[a] Blank corrected EC results ($\mu g/cm^2$) for a 1.5 cm^2 punch from the filter;

[b] total EC on filter calculated as: (EC on sample portion, $\mu g/cm^2$) x total deposit area of the filter (8.55 cm^2);

[c] CNT concentration: total EC on filter per liter of sampled air;

[d] all upstream and downstream EC data were converted to mass per cubic meter air ($\mu g/m^3$).